

Sub-Rayleigh Quantum Imaging

Vittorio Giovannetti¹, Seth Lloyd², Lorenzo Maccone³, and Jeffrey H. Shapiro²

¹*NEST-CNR-INFM & Scuola Normale Superiore, Piazza dei Cavalieri 7, I-56126, Pisa, Italy.*

²*MIT, Research Laboratory of Electronics, 77 Mass. Ave., Cambridge, MA 02139, USA.*

³*QUIT, Dip. Fisica “A. Volta”, Univ. Pavia, via Bassi 6, I-27100 Pavia, Italy.*

No imaging apparatus can produce perfect images: spatial resolution is limited by the Rayleigh diffraction bound that is a consequence of the imager’s finite spatial extent. We show some N -photon strategies that permit resolution of details that are smaller than this bound, attaining either a $1/\sqrt{N}$ enhancement (standard quantum limit) or a $1/N$ enhancement (Heisenberg limit) over standard techniques. In the incoherent imaging regime, the methods presented are loss resistant, because they can be implemented with classical-state light sources. Our results may be of importance in many applications: microscopy, telescopy, lithography, metrology, *etc.*

Quantum effects have been used successfully to provide resolution enhancement in imaging procedures. Among the many proposals that have been made [1], arguably the most famous is the quantum lithography procedure [2]. All of these methods take advantage of the fact that the de Broglie wavelength of a multi-photon light state is much shorter than the photon’s electromagnetic field wavelength [3]: the light generation, propagation, and detection can be performed at optical wavelengths, where it is simple to manipulate, whereas the quantum correlations in the employed states allow one to perform imaging at the much shorter de Broglie wavelength. Such proposals are then based on light sources of highly entangled or squeezed states, as entanglement or squeezing are necessary to achieve efficient quantum enhancements [4]. If, however, efficiency considerations are dropped, it is also possible to employ classical-state light sources and post-selection at the detection stage to filter desirable quantum states from the classical light [5]. In fact, in many practical situations efficiency considerations do not play any role, as the quantum enhancement is typically of the order of the square root of the number of entangled systems [4], whereas in practical situations the complexity of generating the required quantum states has a much worse scaling. Many post-selection imaging procedures employing only classical light sources have been proposed and analyzed [6, 7, 8, 9, 10, 11, 12, 13, 14, 15, 16, 17, 18], and cover a wide range of interesting situations. Analogous methods have been employed successfully also in fields not directly related to imaging [19].

This Letter discusses how one can achieve a resolution enhancement beyond what the apparatus’ structural limits impose for conventional imaging (i.e., the Rayleigh diffraction bound x_R). In particular we show that employing appropriate light sources together with N -photon coincidence photodetection at the output yields a resolution $\sim x_R/\sqrt{N}$. A resolution $\sim x_R/N$ can also be obtained by introducing, at the lens plane, a device that is opaque when it is illuminated by fewer than N photons. The first type of enhancement—a standard quantum limit for imaging—is an N -photon quantum process, but it is roughly equivalent to the classical procedure of

averaging the arrival positions of N photons that originate from the same point on the object. The second type of enhancement—a Heisenberg bound for imaging—is a quantum phenomenon that derives from treating the N photons as a single field of N -times higher frequency. In the incoherent imaging regime, both methods presented here can tolerate arbitrary amounts of loss at the expense of reduced efficiency but without sacrificing resolution.

We start by reviewing some basics of conventional imaging. Then we discuss coherent and incoherent sub-Rayleigh imaging procedures that attain the standard-quantum limit, and finally we introduce our approach to realizing the Heisenberg limit for imaging.

Rayleigh bound:— Consider monochromatic imaging using a circular-pupil thin lens of radius R and focal length f that is placed at a distance D_o from an object of surface area \mathcal{A} , and at a distance D_i from the image plane, where $1/D_o + 1/D_i = 1/f$. In conventional imaging, the object is illuminated by an appropriate (spatially coherent or incoherent) source and the image plane distribution of the light intensity, corresponding to the probability of detecting a photon at each image-plane point \vec{r}_i , is recorded. For photodetectors whose spatial-resolution area \mathcal{S} and temporal-resolution time Δt are sufficiently small, the preceding probability satisfies $P_1(\vec{r}_i) \simeq (\eta \mathcal{S} c \Delta t) \langle E_i^{(-)}(\vec{r}_i, t) E_i^{(+)}(\vec{r}_i, t) \rangle$, where angular brackets denote ensemble average over the illumination’s state, η is the detector quantum efficiency, and $E^{(+)} = [E^{(-)}]^\dagger$ is the positive-frequency component of the electric field. This field component obeys $E_i^{(+)}(\vec{r}_i, t) = \int d^3\vec{k} \mathcal{E}_i^{(+)}(\vec{r}_i; \vec{k}) e^{-ikt/c} a(\vec{k})$, where $a(\vec{k})$ is the field annihilation operator for the optical mode with wave vector \vec{k} , and $\mathcal{E}_i^{(+)}$ is the solution to the associated Helmholtz equation at the image plane. The latter can be written in terms of the corresponding object-plane field $\mathcal{E}_o^{(+)}(\vec{r}_o, \vec{k}) = e^{i\vec{k}_t \cdot \vec{r}_o}$, where \vec{k}_t is the transverse component of \vec{k} , using classical imaging equations. For monochromatic light in the paraxial regime $k_t \ll k$, it follows that [20, 21]

$$\mathcal{E}_i^{(+)}(\vec{r}_i; \vec{k}) = \int \frac{d^2\vec{r}_o}{\mathcal{A}} A(\vec{r}_o) h(\vec{r}_i, \vec{r}_o) \mathcal{E}_o^{(+)}(\vec{r}_o; \vec{k}), \quad (1)$$

where \vec{r}_i and \vec{r}_o are two-dimensional vectors in the image and object planes, $A(\vec{r}_o)$ is the object aperture function [23], and $h(\vec{r}_i, \vec{r}_o)$ is the point-spread function of the imaging apparatus given by [13, 20, 21]

$$h(\vec{r}_i, \vec{r}_o) = \frac{R^2 k^2 A}{4\pi D_o D_i} e^{i\vartheta} \text{somb}(R k |\vec{r}_o + \vec{r}_i/m|/D_o), \quad (2)$$

with $\text{somb}(x) \equiv 2J_1(x)/x$ being the well known Airy function, and $m = D_i/D_o$ being the image magnification factor. In Eq. (2), ϑ is a phase factor which can be generally neglected or compensated.

Incoherent imaging occurs when the object is illuminated by independent (monochromatic) beams propagating from all directions, whence

$$P_1^{(\text{inc})}(\vec{r}_i) = \frac{\eta S c \Delta t}{2\pi k^2 A} I_o \int \frac{d^2 \vec{r}_o}{A} \left| A(\vec{r}_o) h(\vec{r}_i, \vec{r}_o) \right|^2, \quad (3)$$

with $I_o \equiv \langle E_o^{(-)} E_o^{(+)} \rangle$ being the field intensity on the object plane. Coherent imaging prevails when collimated coherent-state illumination is employed, giving rise to

$$P_1^{(c)}(\vec{r}_i) = \eta S c \Delta t I_o \left| \int \frac{d^2 \vec{r}_o}{A} A(\vec{r}_o) h(\vec{r}_i, \vec{r}_o) \right|^2. \quad (4)$$

When the lens radius R is sufficiently large, Eqs. (3) and (4) produce inverted, magnified, perfect images of the object, because $R^2 \text{somb}(R|\vec{x}|) \rightarrow 4\pi \delta^{(2)}(\vec{x})$ for $R \rightarrow \infty$ [20]. For R insufficient to reach this asymptotic behavior, the convolution integrals in Eqs. (3) and (4) produce blurred images. The amount of blurring can be gauged through the Rayleigh diffraction bound: for a point source at \vec{r}_o in the object plane, the resulting image-plane intensity is proportional to $\text{somb}^2(Rk|\vec{r}_o + \vec{r}_i/m|/D_o)$, which comprises a pattern of circular fringes in \vec{r}_i that are centered on $-m\vec{r}_o$. The radius of the first fringe [21],

$$x_R \simeq 0.61 \times 2\pi m D_o / (kR), \quad (5)$$

about $-m\vec{r}_o$ encloses $\sim 84\%$ of the light falling on the image plane. Intuitively, the image of an extended object is then a weighted superposition of radius- x_R circles of centered about each $-m\vec{r}_o$. This is the Rayleigh diffraction bound; using conventional imaging techniques one cannot resolve details smaller than x_R .

Standard quantum limit:— The main idea of sub-Rayleigh imaging is to use an appropriate light source and to replace intensity measurement with spatially-resolving N -fold coincidence detection strategies. Specifically we will focus on the probability of detecting N photons at position \vec{r}_i on the image plane [22], i.e.,

$$P_N(\vec{r}_i) \simeq \frac{(\eta S c \Delta t)^N}{N!} \langle [E_i^{(-)}(\vec{r}_i, t)]^N [E_i^{(+)}(\vec{r}_i, t)]^N \rangle, \quad (6)$$

which can be accomplished by means of doppleron absorbers [24], photon-number resolving detectors, or N -fold coincidence counting. The last two approaches are more convenient than the first, as they exploit the full

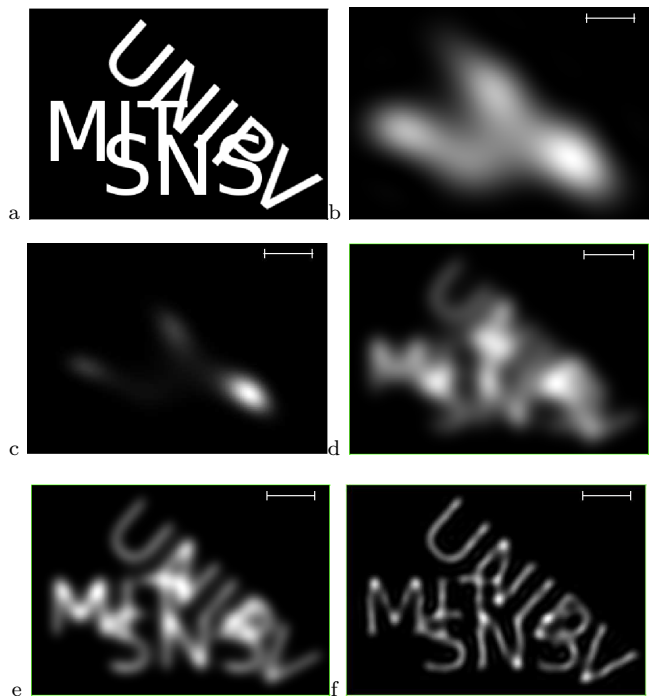


FIG. 1: Comparison of conventional, standard quantum limit, and Heisenberg limit coherent-imaging for a case in which the Rayleigh bound is unable to resolve any object details. (a) Object to be imaged. (b) Conventional coherent image computed for $D_o/R = 250$, $m = 1$, and $k = 6000$. The length scale for \vec{k} is given by the image width, and the segment in the top right corner is the Rayleigh bound x_R . Owing to diffraction, no object details are discernible in the image. (c) N -fold coincidence detection ($N = 5$) with coherent illumination, i.e., the reconstruction through Eq. (7). No resolution enhancement over the previous case occurs despite the N th-order compression of the point-spread function. (d) Standard-quantum-limit reconstruction with illumination by the superposition of Fock states from Eq. (8) with $N = 5$ and $\Delta k_t = 600$. Sub-Rayleigh resolution is present. (e) The same as (d) except that $N = 10$; more resolution enhancement occurs. (f) Heisenberg-limited coherent reconstruction from Eq. (12) with $N = 5$; still further enhancement is evident.

photon statistics so that the N value need not be predetermined. Note that multi-photon detection alone does not guarantee sub-Rayleigh performance. In fact, for the coherent imaging of Eq. (4), N -photon detection gives

$$P_N(\vec{r}_i) = \frac{1}{N!} \left[P_1^{(c)}(\vec{r}_i) \right]^N. \quad (7)$$

Here, the factor of N in the exponent gives an N -fold compression of the fringes in the point-spread function. This compression, however, is not intrinsically quantum. It amounts to taking the N th power of the light intensity, which is simply a classical post-processing of the signal in Eq. (4). Thus no resolution enhancement is obtained through simple N -photon detection, see Fig. 1(c).

As our first example of a source that can be used to

beat the Rayleigh bound, consider an input state that is the superposition of N -photon Fock states that have been focused to a small area $s \equiv (\pi\Delta k_t^2)^{-1} \ll \mathcal{A}$ centered at positions \vec{r}_o on the object plane, viz.,

$$|\psi\rangle \equiv \frac{1}{\sqrt{\mathcal{M}}} \int d^2\vec{r}_o |N\rangle_{\vec{r}_o}, \quad |N\rangle_{\vec{r}_o} \equiv \frac{1}{\sqrt{N!}} [b^\dagger(\vec{r}_o)]^N |0\rangle, \quad (8)$$

where $b(\vec{r}_o)$ is the annihilator of the associated localized spatial mode [25] and $\mathcal{M} \simeq \frac{16\pi\mathcal{A}}{\Delta k_t^2}$ is a normalization constant. Inserting this state into Eq. (6), we find

$$P_N(\vec{r}_i) \simeq \frac{\Delta k_t^2 \mathcal{A}}{16\pi} \xi^N \left| \int \frac{d^2\vec{r}_o}{\mathcal{A}} Q^N(\vec{r}_i, \vec{r}_o) \right|^2, \quad (9)$$

$$Q(\vec{r}_i, \vec{r}_o) \equiv \int \frac{d^2\vec{r}}{\mathcal{A}} A(\vec{r}) h(\vec{r}_i, \vec{r}) F_{\Delta k_t}(|\vec{r}_o - \vec{r}|),$$

where $F_{\Delta k_t}(x) \equiv \pi\Delta k_t^2 \mathcal{A} \text{somb}(\Delta k_t x/2)$, and $\xi \equiv \eta \frac{\Delta\omega\Delta t}{\pi\Delta k_t^2 \mathcal{A}} \frac{S}{\mathcal{A}}$ is a dimensionless quantity that is typically very small because of the monochromatic ($\Delta\omega\Delta t \ll 1$) and focusing assumptions ($\pi\Delta k_t^2 \mathcal{A} \gg 1$). Equation (9) can be simplified by assuming $D_o/R \gg k/\Delta k_t$, which implies that each number state in the superposition is focused to a spot much smaller than the object-plane Rayleigh limit of the lens. In this case h can be extracted from the integral yielding $Q(\vec{r}_i, \vec{r}_o) \simeq h(\vec{r}_i, \vec{r}_o) \tilde{A}(\vec{r}_o)$ with $\tilde{A}(\vec{r}_o) \equiv \int \frac{d^2\vec{r}}{\mathcal{A}} A(\vec{r}) F_{\Delta k_t}(|\vec{r}_o - \vec{r}|)$. Now Eq. (9) becomes

$$P_N^{(c)}(\vec{r}_i) \simeq \frac{\Delta k_t^2 \mathcal{A}}{16\pi} \xi^N \left| \int \frac{d^2\vec{r}_o}{\mathcal{A}} [\tilde{A}(\vec{r}_o) h(\vec{r}_i, \vec{r}_o)]^N \right|^2, \quad (10)$$

which, contrary to Eq. (7), cannot be obtained through post-processing of P_1 , and which generalizes coherent imaging (4) to N -photon detection. The point-spread function that governs spatial resolution is now h^N —which is narrower than h —so that when $A(\vec{r}_o) \simeq \tilde{A}(\vec{r}_o)$ there is an enhancement in resolution over the Rayleigh bound. More generally, even if A and \tilde{A} differ significantly, one can still beat the Rayleigh bound if N is sufficiently large and $D_i/R \gg k/\Delta k_t$, see Figs. 1(d) and (e).

An analogous generalization for incoherent imaging is obtained by replacing the state Eq. (8) with an incoherent mixture of focused Fock states, i.e., $\rho = \int \frac{d^2\vec{r}_o}{\mathcal{A}} |N\rangle_{\vec{r}_o} \langle N|$. In this case Eq. (10) becomes

$$P_N^{(\text{inc})}(\vec{r}_i) \simeq \xi^N \int \frac{d^2\vec{r}_o}{\mathcal{A}} |\tilde{A}(\vec{r}_o)|^{2N} |h(\vec{r}_i, \vec{r}_o)|^{2N}, \quad (11)$$

which generalizes Eq. (3) to N -photon detection. The corresponding resolution enhancement is shown in Fig. 2.

The states employed in Eqs. (8) and (11) are highly sensitive to loss. Nevertheless, N -fold incoherent imaging can be realized with loss-resistant light sources. Suppose we use an incoherent mixture of coherent states that randomly illuminate all points on the object: $\sigma = \int \frac{d^2\vec{r}_o}{\mathcal{A}} |\alpha\rangle_{\vec{r}_o} \langle \alpha|$, where $|\alpha\rangle_{\vec{r}_o} \equiv \exp[\alpha b^\dagger(\vec{r}_o) - \alpha^* b(\vec{r}_o)] |0\rangle$.

Equation (11) still applies with an extra multiplicative factor of $|\alpha|^{2N}/N!$ to account for the Poissonian photodetection statistics of coherent states. The state σ can be prepared by shining a highly-focused laser beam on the object, one point at the time. This state is highly robust to loss, because loss parameter μ just takes $|\alpha\rangle$ into $|\sqrt{\mu}\alpha\rangle$. Hence an arbitrary amount of loss can be tolerated—without sacrificing resolution—simply by increasing $|\alpha|$.

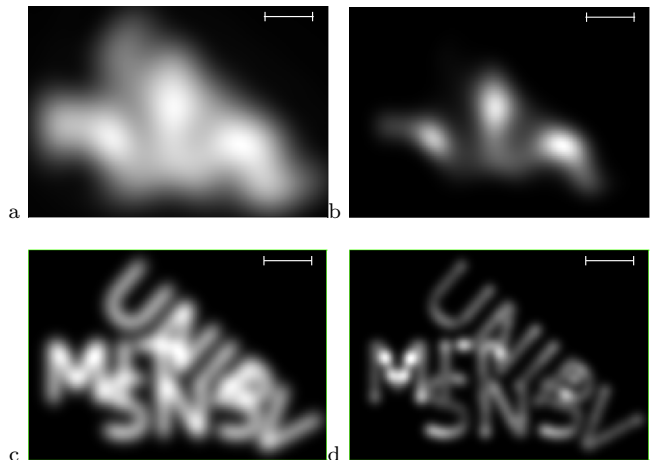


FIG. 2: Comparison of conventional and standard quantum limit incoherent imaging of the object shown in Fig. 1(a) with the same $D_o/R = 250$, $m = 1$, and $k = 6000$. (a) and (b) Conventional images from Eq. (7) with $N = 1$ and 5 , respectively. The images are featureless blurs, because the Rayleigh bound x_R is unable to resolve any object details. (c) and (d) Reconstruction via Eq. (11) using the state σ for $N = 5$ and 10 , respectively, with $\Delta k_t = 600$. An obvious increase in resolution is seen.

The improved resolution afforded by the procedures detailed above can be roughly estimated by gauging by narrowing of the point-spread function h that results from taking its N th power. This can be done, for instance, by evaluating the radius $x_R(N)$ that contains 84% of the area under somb^{2N} in the plane. Numerical analysis shows that $x_R(N)/x_R \sim 1/\sqrt{N}$, which suggests a standard quantum limit [1] for imaging. This should be taken only as a rough estimate, as $x_R(N)$ is also the radial dimension of a point-like object imaged using the post-processing strategy of Eq. (7). For more extended objects, the actual resolution enhancement will also depend on Δk_t . The $1/\sqrt{N}$ scaling exposes the classical nature of this enhancement: the same effect can be attained by averaging the arrival positions of N photons at the image plane. This is surely advantageous over N -photon detection in many situations, but it is impractical for lithography or film photography, and it seems impossible to classically reproduce the coherent imaging case of Eq. (10). In addition, from general principles [1, 4] one would expect the ultimate bound (a Heisenberg limit for

imaging) to have $1/N$, scaling, i.e., a resolution $\sim x_R/N$, which is not achievable with classical strategies.

Heisenberg limit:— The Heisenberg $1/N$ scaling can be obtained by treating the N photons as a single entity of N -times higher frequency. This situation can be simulated, at least in principle, by inserting immediately in front of the lens a screen divided into small sections each of area s_F such that if less than N photons reach one section, they are absorbed, otherwise they are coherently transmitted. Such a screen does not currently exist, but in principle one could be built, e.g., by using doppleron materials [24]. Then, if the object is illuminated by the focused coherent states described above, only N photons that originate at \vec{r}_o , successfully transit the screen within one of its area- s_F segments, and get detected at \vec{r}_i can contribute to the image at that point. In this case, the operators $[E_i^{(+)}(\vec{r}_i, t)]^N$ of the N -photon absorption probability (10) are approximately [26]

$$[E_i^{(+)}(\vec{r}_i, t)]^N \simeq \gamma \int \frac{d^2 \vec{r}_o}{A} [\tilde{A}(\vec{r}_o)]^N h_N(\vec{r}_i, \vec{r}_o) [b(\vec{r}_o)]^N. \quad (12)$$

Here: h_N is obtained from Eq. (2) by replacing k with Nk , i.e., h_N is the point-spread function for photons having N -times higher frequency than the illumination; and γ accounts for the spatial resolution of the doppleron screen, i.e., it is of order $(\frac{s_F}{\pi R^2})^N$. Equation (12) describes the absorption of N frequency- ω photons that originated near \vec{r}_o and then propagated through the imaging apparatus as if they were a single frequency- $N\omega$ photon. It gives rise to coherent and incoherent images that are formally equivalent to those of Eqs. (4) and (3) for a light beam of wave number Nk , thus realizing the Heisenberg limit of an N -fold resolution improvement over the Rayleigh bound, see Fig. 1(f). This method shows that Heisenberg-limited resolution can be obtained using classical light, albeit with an even worse efficiency than the N -photon detection methods given above.

This research was supported in part by the W. M. Keck Foundation for Extreme Quantum Information Theory and by the DARPA Quantum Sensors Program.

-
- [1] For a recent review, see V. Giovannetti, S. Lloyd, and L. Maccone, *Science* **306**, 1330 (2004).
 [2] A. N. Boto, *et al.*, *Phys. Rev. Lett.* **85**, 2733 (2000).
 [3] J. Jacobson, G. Björk, I. Chuang, and Y. Yamamoto, *Phys. Rev. Lett.* **74**, 4835 (1995).
 [4] V. Giovannetti, S. Lloyd, L. Maccone, *Phys. Rev. Lett.* **96**, 010401 (2006); S. L. Braunstein, *Nature* **440**, 617 (2006).
 [5] K. L. Pregnell and D. T. Pegg, *J. Mod. Opt.* **51**, 1613 (2004).
 [6] H. P. Yuen and J. H. Shapiro, *IEEE Trans. Inf. Th.* **24**, 657 (1978).

- [7] P. R. Hemmer, A. Muthukrishnan, M. O. Scully, and M. S. Zubairy, *Phys. Rev. Lett.* **96**, 163603 (2006); A. Muthukrishnan, M. O. Scully, and M. S. Zubairy, *J. Opt. B: Quantum Semiclass. Opt.* **6**, S575 (2004).
 [8] D. Korobkin, and E. Yablonovitch, *Opt. Eng.* **41**, 1729 (2002).
 [9] C. Thiel, T. Bastin, J. Martin, E. Solano, J. von Zanthier, and G. S. Agarwal, *quant-ph/070.1024* (2007).
 [10] S. J. Bentley and R. W. Boyd, *Opt. Exp.* **12**, 5735 (2004).
 [11] M. Zhang, Q. Wei, X. Shen, Y. Liu, H. Liu, Y. Bai, and S. Han, *Phys. Lett. A* in press, *quant-ph/0612060* (2006).
 [12] K. Wang, and D.-Z. Cao, *Phys. Rev. A* **70**, 041801(R) (2004).
 [13] Y. Shih, *IEEE J. Sel. Topics in Quantum Electron.* **13**, 1016 (2007).
 [14] E. Yablonovitch and R. B. Vrijen, *Opt. Eng.* **38**, 334 (1999).
 [15] A. Pe'er, *et al.*, *Opt. Express* **12**, 6600 (2004).
 [16] B. I. Erkmen, J. H. Shapiro, *Phys. Rev. A* **77**, 043809 (2008).
 [17] M. I. Kolobov (Ed.) *Quantum Imaging*, (Springer, New York, 2006).
 [18] L. A. Lugiato, A. Gatti and E. Brambilla, *J. Opt. B: Quantum Semiclass. Opt.* **4**, S176 (2002).
 [19] F. S. Cataliotti, R. Scheunemann, T. W. Hänsch, and M. Weitz, *Phys. Rev. Lett.* **87**, 113601 (2001); C. Skornia, J. von Zanthier, G. S. Agarwal, E. Werner, and H. Walther, *Phys. Rev. A* **64**, 063801 (2001); M. W. Mitchell, J. S. Lundeen, and A. M. Steinberg, *Nature (London)* **429**, 161 (2004); K. J. Resch, K. L. Pregnell, R. Prevedel, A. Gilchrist, G. J. Pryde, J. L. O'Brien, and A. G. White, *Phys. Rev. Lett.* **98**, 223601 (2007).
 [20] J. W. Goodman, *Introduction to Fourier optics* (McGraw-Hill, New York, 1988).
 [21] M. Born and E. Wolf, *Principles of optics* (Cambridge Univ. Press, Cambridge, 1999).
 [22] L. Mandel and E. Wolf *Optical Coherence and Quantum Optics* (Cambridge Univ. Press, Cambridge, 1995).
 [23] The function A measures the attenuation of the impinging light due to the object. Here we assume A to be independent of \vec{k} ; the generalization to a wave-vector dependent A is straightforward.
 [24] J. J. Tollett, *et al.*, *Phys. Rev. Lett.* **65**, 559 (1990); N. P. Bigelow and M. G. Prentiss, *Phys. Rev. Lett.* **65**, 555 (1990).
 [25] It is given by $b(\vec{r}_o) \equiv \int \frac{d\omega}{\sqrt{\Delta\omega}} \int \frac{d^2 \vec{k}_t}{\sqrt{\pi \Delta k_t^2}} e^{i\vec{k}_t \cdot \vec{r}_o} a(\vec{k})$, where the frequency integration is performed over a small bandwidth $\Delta\omega$ around the mean frequency $\omega = kc$ and the wave-vector integration is performed over $|k_t| \leq \Delta k_t$. The exact expression for \mathcal{M} is $\int d^2 \vec{r}_o \int d^2 \vec{r}_o' F_{\Delta k_t^2}^N (|\vec{r}_o - \vec{r}_o'|) / A^N$, which, for highly localized modes $\pi \Delta k_t^2 A \ll 1$, gives $\mathcal{M} \simeq \frac{16\pi A}{\Delta k_t^2}$.
 [26] Use the screen-to-lens transfer function to write $[E_i^{(+)}(\vec{r}_i, t)]^N$ as a convolution of the products $E_\ell^{(+)}(\vec{r}_\ell^{(1)}, t) \dots E_\ell^{(+)}(\vec{r}_\ell^{(N)}, t)$, with $E_\ell^{(+)}(\vec{r}_\ell, t)$ being the electric field on the screen. The screen removes all contributions save those for which the $\vec{r}_\ell^{(j)}$ fall in the same area- s_F region. Equation (12) follows by writing the resulting operator as a convolution of $E_o^{(+)}(\vec{r}_o^{(1)}, t) \dots E_o^{(+)}(\vec{r}_o^{(N)}, t)$ through the object-to-lens transfer function, and by noticing that for focused sources it can be approximated by $[b(\vec{r}_o^{(1)})]^N$.